Interaction of Cl_2 with Fe(110) in the Temperature Range 90-1050 K

A. L. Linsebigler, V. S. Smentkowski, M. D. Ellison, and J. T. Yates, Jr.*

Contribution from the Surface Science Center, Department of Chemistry, University of Pittsburgh, Pittsburgh, Pennsylvania 15260. *Received June 28, 1991*

Abstract: Temperature-programmed desorption and Auger spectroscopic measurements were utilized in this work to study the interaction of Cl_2 with Fe(110) in the temperature range 90-1050 K. Irreversible dissociative Cl_2 adsorption initially occurs at 90 K and results in the oxidation of the Fe(110) surface. This dissociative adsorption process is followed by chlorine adsorption at 90 K which produces desorption states for Cl_2 from a weakly chemisorbed chlorine layer (117 K) and from the multilayer (112 K). In addition, there is produced $FeCl_2$ from both a zero-order desorption kinetics state (560 K) and a broad desorption state ($580 < T < 750$ K), and a high-temperature iron chloride species which desorbs above 900 K. Cl_2 adsorbs dissociatively and irreversibly at 298 K causing oxidation of the iron surface and $FeCl_2$ production. Artificial defect production on the iron surface leads to an increase in the zero-order $FeCl_2$ yield, indicating that clustering of $FeCl_2$ occurs at defect sites producing $FeCl_2$ clusters of order 5 Å or larger in thickness. The kinetics of $FeCl_2$ production are strongly dependent on the temperature of Cl_2 adsorption. The results obtained for the Cl_2/Fe(110) system are compared to previous systems studied, CCl_4/Fe(110), C_2Cl_4/Fe(110), and CCl_2F_2/Fe(110).

I. Introduction

The corrosive nature of chlorine and the high chemical reactivity of iron make the interaction of these elements an important surface chemical system for study. Despite the fundamental and technological importance of this system, there have been only three experimental papers published concerning surface science investigations of the interaction of chlorine with atomically clean single crystalline[1,2] and polycrystalline[2] iron surfaces.

The interaction of Cl_2 with Fe(100) was studied by Dowben and Jones at 300 K.[1] In this work, the saturation Cl coverage was defined as 0.75 Cl atoms per 4-fold site, where the 4-fold site was defined as a unit of area and was not meant to imply that an adatom was adsorbed in that position.

Work function measurements showed that increasing the quantity of adsorbed chlorine on Fe(100) increased the work function up to a maximum increase of 1.43 eV at saturation, consistent with an outward oriented negative dipole. Comparing the work function measurements to coverage measurements made by Auger spectroscopy showed that the work function increases monotonically with chlorine coverage.

LEED measurements on Fe(100) as a function of chlorine coverage and as a function of heating in the temperature range 395-675 K indicated that a series of surface phases exist in this temperature range.

The intensity of the Cl(LMM) Auger transition as a function of temperature for the saturated Fe(100) crystal was studied. Up to a temperature of ~445 K there was almost no decrease in chlorine Auger intensity. However, in the temperature range 445-520 K, the rate of decrease in the chlorine Auger intensity slowly increased with increasing temperature. Above ~520 K, the rate of chlorine loss became substantial and remained virtually constant up to a temperature of 735 K (the highest temperature studied).

No desorption products were detected in the non line-of-sight thermal desorption measurements. As a result, it was postulated that the chlorine was desorbing as Cl atoms or diffusing into the bulk at high temperatures. The detector geometry used in this work on Fe(100) would not be capable of detecting the formation of a volatile iron chloride species.

Hino and Lambert studied the interaction of Cl_2 with polycrystalline iron at 300 K.[2] Work function and Auger measurements were used to monitor the chlorine adsorption by the surface. Both methods showed that the chlorine coverage increased rapidly with increasing Cl_2 exposure up to 1.1×10^{15} Cl_2/cm^2. At higher exposures there was a much slower rate of adsorption.

Thermal desorption measurements obtained from the interaction of Cl_2 with polycrystalline iron at 300 K revealed $FeCl_2$ desorption. For low Cl_2 exposures (1.4×10^{14} Cl_2/cm^2), a single $FeCl_2$ desorption process was observed at temperatures greater than ~900 K. Increasing the Cl_2 exposure to 1.1×10^{15} Cl_2/cm^2 caused the onset desorption temperature for $FeCl_2$ to decrease as the quantity of desorbing $FeCl_2$ increased. For Cl_2 exposures greater than 1.1×10^{15} Cl_2/cm^2, a second $FeCl_2$ desorption process was observed at 550 K. Increasing the Cl_2 exposure (up to 6.7×10^{15} Cl_2/cm^2) increased the yield of the $FeCl_2$ desorption process at 550 K, while the yield of the high-temperature $FeCl_2$ desorption process remained essentially constant. The leading edges of the 550 K $FeCl_2$ desorption spectra accurately overlap, indicating that this desorption process occurs via zero-order kinetics, consistent with a model in which the 550 K $FeCl_2$ state originates from the sublimation of bulk $FeCl_2$.

Hino and Lambert also conducted ultraviolet and X-ray photoelectron spectroscopy (UPS and XPS, respectively) on an Fe(100) single-crystal surface exposed to chlorine.[2] He I UP spectra obtained at low exposures of chlorine to the Fe(100) surface showed the appearance of a 6-eV Cl(3p) derived peak that increases in intensity with increasing chlorine exposure. This Cl(3p) derived peak is a common feature in metal-Cl chemisorption systems. At higher chlorine exposures additional features occur between 4 and 9 eV on either side of the Cl(3p) derived peak. These features agree with reported spectra of gaseous $FeCl_2$.[2]

An XP spectrum of Fe(2p) for a clean Fe(100) surface is characterized by strong $2p_{3/2}$ and $2p_{1/2}$ peaks at binding energies of 706.5 and 720.4 eV, respectively. After a chlorine exposure of 4×10^{18} Cl_2/cm^2 at 300 K, the XP spectrum of Fe(2p) showed a new feature 3.2 ± 0.5 eV above the 2p peaks. Increasing the grazing angle of electron emission enhanced the new feature on the high binding energy side of the 2p peaks as would be expected for an $FeCl_2$ layer.

In this work, we report studies of the interaction of Cl_2 with a Fe(110) single crystal. Adsorption studies at both 90 and 300 K have been carried out using Auger spectroscopy and temperature-programmed desorption spectroscopy. Quantitative correlation between known Cl_2 exposures and the two surface spectroscopies were made. In addition, the role of artifically induced surface defects on the behavior of Fe(110) in its interaction with Cl_2 has been investigated.

II. Experimental Section

The ultrahigh vacuum system used in this work was previously described in detail elsewhere.[3,4] Briefly, the stainless steel chamber con-

(1) (a) Dowben, P. A.; Jones, R. G. *Surf. Sci.* **1979**, *84*, 449. Also see a theoretical paper related to these experiments: (b) Debnath, N. C.; Anderson, A. B. *J. Vac. Sci. Technol.* **1982**, *26*, 945. (c) Mueller, D. R.; Rhodin, T. N.; Sakisaka, Y.; Dowben, P. A. *Surf. Sci.* **1991**, *250*, 185.

(2) Hino, S.; Lambert, R. M. *Langmuir* **1986**, *2*, 147 and references therein.

0002-7863/92/1514-465$03.00/0

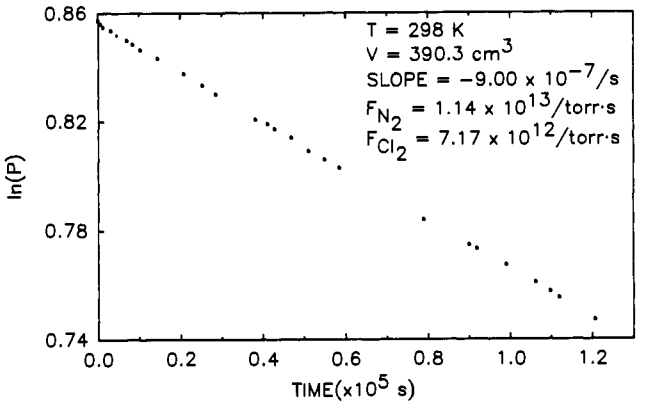

Figure 1. Plot of ln (P) vs time (s) for N_2(g). The conductance of the collimated beam doser was calculated from the slope of the plot.

tains an off-axis Leybold-Heraeus IQE 10/35 ion source for sputtering the crystal at an incident angle of 68°, a Perkin-Elmer single pass CMA digital Auger spectrometer, and a UTI 100C quadrupole mass spectrometer (QMS) located in a differentially pumped shield containing a 0.2-cm-diameter coaxial sampling aperture for line-of-sight desorption measurements from the center of the 0.50-cm-diameter crystal. A Teknivent/Vector One interface system is used to digitize and multiplex the mass spectral data.

Accurate gas exposures to the crystal surface were obtained using a microcapillary array collimated beam doser[5-7] positioned at a reproducible crystal-to-doser distance of 0.80 cm. Conductance through the doser was controlled by a 6-μm pinhole aperture.

To assure accurate gas exposures to the crystal surface, the collimated beam doser was calibrated with N_2(g) using standard volumetric methods.[8-10] The pressure drop in the gas handling system (V = 390.3 cm^3) was measured with a 0–10 Torr Baratron capacitance manometer for an extended time period at 298 K. Figure 1 shows a plot of ln (P) vs time for N_2(g). The slope of this plot is used to measure the conductance of the collimated beam doser, and Knudsen effusion[11] was assumed to apply at the 6-μm aperture, permitting the conductance for Cl_2 to be evaluated on the basis of the measurements with N_2(g). The first three data points of Figure 1 indicate a transient behavior in the high-pressure section of the gas handling system and are not utilized in the determination of the slope. A fractional interception factor of 0.18 was calculated from the known crystal-to-doser geometry.[6] On the basis of a propagation of error analysis involving all experimental variables, the exposure of Cl_2 molecules on the crystal could be measured with an estimated accuracy of ±9%.

For thermal desorption measurements, the Fe(110) crystal could be accurately placed 1.00 mm away from the sampling aperture in the QMS shield.[3] Extraneous gas molecules desorbing from the edges of the crystal, the heating leads, the thermocouple, and the copper support assembly are eliminated by this procedure.

The temperature-programmed desorption (TPD) experiments were carried out using a digital temperature programmer[12] which resistively heated the crystal at a rate of 2.2 deg K/s. The crystal temperature was measured using a 0.006-cm-diameter chromel–alumel thermocouple spot welded to the back of the crystal.

The initial preparation and cleaning of the Fe(110) single crystal has been described in detail elsewhere.[4] To obtain a clean crystal, extensive ion bombardment and annealing are required. Auger spectroscopy determined that the surface of the crystal remained free of impurities for heating below 1000 K. When the crystal was heated to 1030 K for ~15 min, sulfur slowly diffused to the surface of the crystal from the bulk.

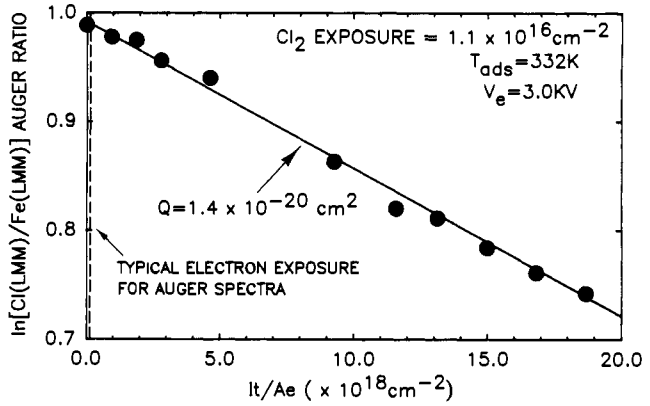

Figure 2. Plot of ln [Cl/Fe] Auger ratio vs It/Ae following adsorption of 1.1 × 10^{16} Cl_2/cm^2. The cross section for loss of Cl is 1.4 × 10^{-20} cm^2. Note, the plot indicates that the reduction in the Cl/Fe ratio due to electron beam effects is negligible when typical Auger spectroscopy data acquisition conditions are employed.

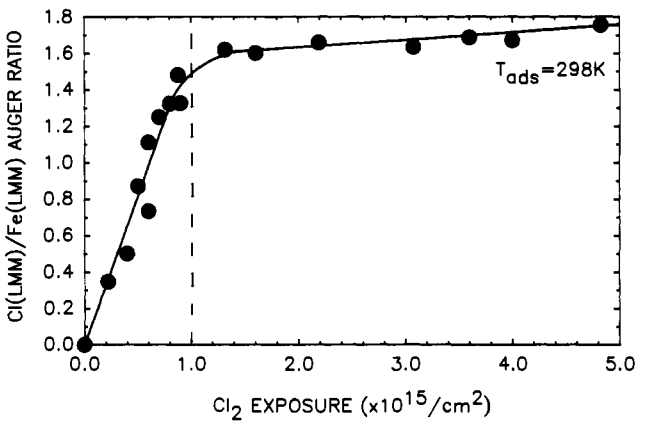

Figure 3. Plot of Cl(LMM)/Fe(LMM) Auger ratio as a function of Cl_2 exposure on Fe(110) at 298 K. The dashed vertical line indicates the completion of one monolayer of adsorbed Cl_2.

Prior to the start of each experiment, the Fe(110) crystal was cleaned by Ar^+ sputtering using a 2.5-kV beam at a current of ~1.9 × 10^{-6} A for ~15 min, followed by annealing the crystal at 700 K for ~5 min. An Auger spectrum was obtained to confirm the production of a clean Fe(110) crystal surface.

Auger spectroscopy experiments were used to characterize the adsorption of Cl_2 on the Fe(110) surface. At 90 K, multilayers of molecular Cl_2 physisorb on the iron surface and Auger spectroscopy experiments show the occurrence of significant ESD (electron stimulated desorption) effects. Thus Auger spectroscopy was not employed in the multilayer situation. In contrast to the multilayer behavior, we have shown (Figure 2) that Auger spectroscopy may be effectively employed to study the monolayer of adsorbed Cl at 332 K without concern for ESD effects. The cross section evaluated for the loss of Cl during electron bombardment for long periods of time is 1.4 × 10^{-20} cm^2, as shown in Figure 2. Using typical data acquisition conditions (a 3-kV electron beam current of 1.5 × 10^{-6} A, a measured electron beam diameter of 0.085 cm, and an acquisition time of 70 s) the electron exposure for the acquisition of an Auger spectrum is 1.2 × 10^{17} e/cm^2. As shown in Figure 2, this corresponds to only a 0.16% reduction in the Cl(LMM)/Fe(LMM) ratio which is negligible using the Auger acquisition conditions mentioned above. For sequential measurements of Auger intensity, the crystal was translated 0.1 cm between measurements to avoid cumulative beam damage effects.

Chlorine (99.99% minimum purity) was obtained in a break seal flask from Matheson and was used without further purification. Wall effects were observed when the freshly baked gas line of the dosing system was filled with Cl_2 which caused the pressure in the gas line to decrease at an initial rate of 0.3 %/min as monitored by the baratron pressure gauge. To eliminate the problem, the following experimental sequence was performed: (1) the gas line was filled with 10 Torr of Cl_2; (2) the Cl_2 was allowed to sit in the gas line system for ~20 h; (3) the gas line was pumped out; and (4) the gas line was refilled with fresh Cl_2 to a pressure of 4 Torr. Following this procedure, the Cl_2 pressure remained constant in the gas line.

(3) Smentkowski, V. S.; Yates, J. T., Jr. *J. Vac. Sci. Technol.* **1989**, *A7*(6), 3325.
(4) Smentkowski, V. S.; Cheng, C. C.; Yates, J. T., Jr. *Langmuir* **1990**, *6*, 147.
(5) Bozack, M. J.; Muehlhoff, L.; Russell, J. N., Jr.; Choyke, W. J.; Yates, J. T., Jr. *J. Vac. Sci. Technol.* **1987**, *A5*, 1.
(6) Winkler, A.; Yates, J. T., Jr. *J. Vac. Sci. Technol.* **1988**, *A6* (5), 2929.
(7) Campbell, C. T.; Valone, S. M. *J. Vac. Sci. Technol.* **1985**, *A3* (2), 408.
(8) Madey, T. E. *Surf. Sci.* **1972**, *33*, 355.
(9) Yates, J. T., Jr. *Methods of Exp. Phys.* **1985**, *22*, 425.
(10) Dresser, M. J.; Taylor, P. A.; Wallace, R. M.; Choyke, W. J.; Yates, J. T., Jr. *Surf. Sci.* **1989**, *218*, 75.
(11) Atkins, P. W. *Physical Chemistry*, 2nd ed.; W. H. Freeman and Co.: San Francisco, 1982; p 877.
(12) Muha, R. J.; Gates, S. M.; Basu, P.; Yates, J. T., Jr. *Rev. Sci. Instrum.* **1985**, *56*, 613.

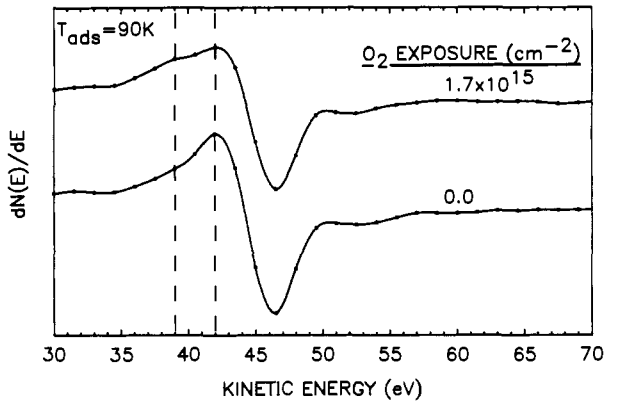

Figure 4. A comparison of the line shape of the Fe(MVV) Auger transition between a clean Fe(110) surface (bottom) and a Fe(110) surface exposed to 1.7×10^{15} O_2/cm^2, at 90 K. Dashed vertical lines indicate energy regions of interest in the Auger line shape.

The internal surfaces of the beam doser were saturated by letting Cl_2 gas pass into the UHV chamber while the 70 amu Cl_2^+ signal was monitored by the mass spectrometer, operating as a residual gas analyzer with a large fitted closure in the QMS shield in its open position.[3] Upon admitting the Cl_2 gas to the doser, the 70 amu signal remained constant at its baseline value for ~10 s. The QMS signal then started to slowly increase and reached a steady-state value after ~30 min. Following this procedure, the doser remained saturated throughout all gas dosing procedures employed here.

III. Results

1. Auger Spectroscopic Studies of Chlorine Adsorption on Fe(110). 1.1. Auger Measurements of Cl_2 Adsorption at 298 K on Fe(110). The intensities of the Cl(LMM) and Fe(LMM) Auger transitions were measured as a function of Cl_2 exposure to the iron surface at 298 K as shown in Figure 3. After several Auger intensity measurements were obtained at different Cl_2 exposures in the 0–5 $\times$ 10^{15} Cl_2/cm^2 range, the crystal was sputtered clean and annealed at ~700 K. The same sequence, at different exposures, was then repeated to fill in the data points on the curve which represents a summation of three separate adsorption experiments. The uptake curve in Figure 3 shows a significant change in slope at an exposure of $\sim 1 \times 10^{15}$ Cl_2/cm^2, indicating qualitatively the completion of chemisorbed Cl monolayer formation. The chlorine Auger signal continues to rise slightly as the exposure is increased to 5×10^{15} Cl_2/cm^2. Measurements of this type were not performed at 90 K due to considerable ESD effects from the Auger electron beam on the multilayers of Cl_2 adsorbed on the iron surface.

1.2. Line Shape Changes in the Low-Energy Region of the Iron Auger Spectra. Previous studies of oxygen adsorption on Fe(110)[13] showed line shape changes in the Fe(MVV) transition of the Auger spectrum following oxygen exposure, as shown in Figure 4. The bottom derivative spectrum shows a clean Fe(110) surface and exhibits an Fe(MVV) Auger transition with a negative-going feature at 46.5 eV. The top spectrum shows the same transition with an oxygen exposure of 1.7×10^{15} O_2/cm^2 adsorbed at 90 K. This spectrum exhibits the same negative-going feature at 46.5 eV as observed for the clean Fe(110) surface. The Auger spectrum for the oxygen-exposed surface also exhibits a positive-going feature at 39 eV that is essentially absent for the clean Fe(110) surface. In addition there is an attenuation of the positive-going Auger feature at 42 eV. These line shape changes have been attributed to oxidation of the iron surface from dissociative adsorption of oxygen.[13]

We have employed similar Auger line shape measurements to determine whether Cl_2 chemisorption leads to oxidation of Fe(110). Figure 5 shows the low-energy region of the Fe(MVV) Auger derivative spectrum when chlorine is adsorbed on the iron surface at 326 K. The bottom spectrum shows the clean Fe(110) surface

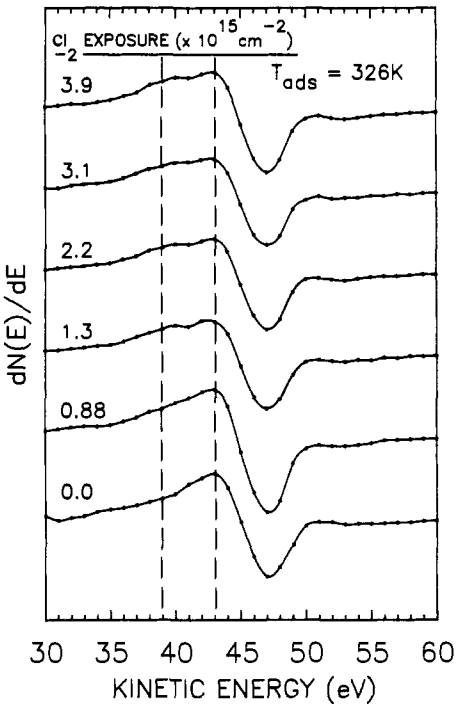

Figure 5. Line shape changes in the Fe(MVV) Auger transition following adsorption of Cl_2 at 326 K. Dashed vertical lines indicate energy regions of interest in the Auger line shape as the Cl_2 exposure is increased.

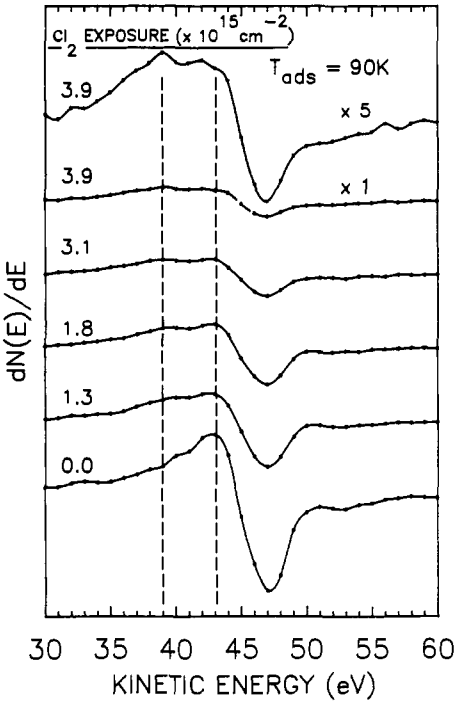

Figure 6. Line shape changes in the Fe(MVV) Auger transition following adsorption of Cl_2 at 90 K. Attenuation occurs as the Cl_2 exposure is increased at 90 K.

which again exhibits the same negative-going feature (at ~47 eV) in the Auger spectrum. With increasing exposure, the Fe(MVV) transition shows an increase in intensity of the positive-going shoulder at 39 eV and an attenuation of the positive-going feature at 43 eV. This Auger line shape change is the same as the line shape change caused by the oxidation of the iron surface due to oxygen adsorption, as shown in Figure 4.[13] We therefore believe, as might be expected, that iron oxidation occurs as a result of dissociative adsorption of Cl_2 at 326 K.

When chlorine is adsorbed on the iron surface at 90 K the Fe(MVV) transition is attenuated as shown in Figure 6. This

(13) Smentkowski, V. S.; Yates, J. T., Jr. *Surf. Sci.* **1990**, *232*, 113.

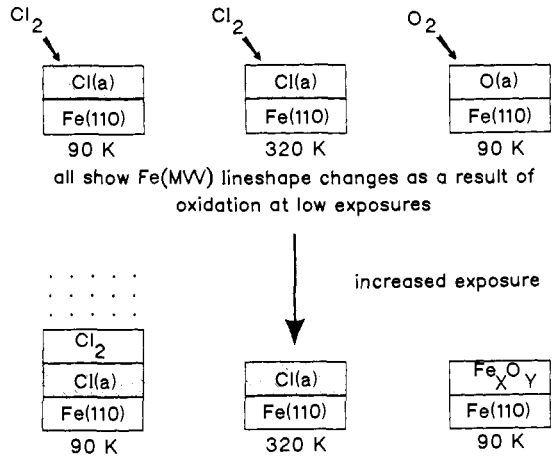

Figure 7. Schematic illustrating oxidation of the Fe(110) surface from adsorption of Cl_2 (at 90 and 320 K) and O_2 (90 K).

attenuation is attributed to the presence of multilayers of Cl_2 that physisorb on the iron surface at 90 K (Cl_2 does not molecularly adsorb at 326 K and hence does not produce a large Fe(MVV) attenuation as shown in Figure 5). When at 90 K the chlorine exposure is increased to 3.9×10^{15} Cl_2/cm^2, the Fe(MVV) transition is almost completely attenuated. Magnification of the Auger spectrum shows clearly that the same positive-going shoulder exhibited at 39 eV and the same attenuation of the positive-going feature at 43 eV are also present at 90 K. *This is therefore indicative that even at 90 K, Cl_2 adsorbs dissociatively in the limit of low coverage and causes oxidation of the Fe(110) surface.* This conclusion should be checked by other spectroscopic methods. The oxidized iron surface is then covered by multilayers of undissociated Cl_2.

1.3. Summary of Oxidation Behavior As Determined by Auger Spectroscopy. A schematic representation of the Fe(110) surface oxidation experiments, under the conditions previously mentioned, is illustrated in Figure 7. At 90 K, using low oxygen exposures, oxygen adsorbs dissociatively, oxidizing the iron surface as indicated by the Fe(MVV) line shape change (Figure 4).[13] Increasing the oxygen exposure leads to the formation of iron oxide species of the type Fe_xO_y, and the details of this process are reported elsewhere.[13] After the adsorption of chlorine on the iron surface, using low Cl_2 exposures at both 90 and 326 K, the Auger spectrum shows a very similar Fe(MVV) line shape change as for oxygen adsorption on the iron surface. This indicates that the oxidation of the iron surface is due to the dissociative adsorption of chlorine at 90 and 326 K. Increasing the chlorine exposure at 90 K attenuates the intensity of the Fe(MVV) transition due to adsorption of multilayers of Cl_2 molecules over the first layer of dissociated Cl atoms. Multilayers of Cl_2 do not adsorb on the iron surface at 326 K.

1.4. Auger Spectroscopic Studies of the Thermal Behavior of Chlorine Layers on Fe(110). The temperature dependence of the intensity for the chlorine Auger signal was monitored following the adsorption of 1.0×10^{16} Cl_2/cm^2 at 90 K. For this experiment, the crystal was heated (2.2 deg K/s) to the desired initial temperature (300 K) where all of the multilayer molecular Cl_2 had desorbed; the crystal was then cooled quickly to 90 K where the Auger spectrum was obtained. The crystal was heated again to the next desired temperature (350 K) and cooled quickly to 90 K to obtain another Auger spectrum. This procedure was continued up to 1000 K, the highest temperature studied. The crystal was also translated 0.1 cm before each Auger spectrum was acquired in order not to resample the same spot on the crystal which had previously been exposed to the electron beam. Each spot on the crystal surface was resampled once, however, leading to a Cl(LMM)/Fe(LMM) ratio reduction by ESD of 0.5% which is negligible. Figure 8 illustrates the existence of two thermally activated surface depletion processes for chlorine. The first depletion process begins around 450 K and ends at 570 K. The culmination of this process near 570 K is attributed to the desorption of $FeCl_2$ (to be shown later via mass spectroscopy). The second surface chlorine depletion process begins near 600 K and continues until 1000 K. This chlorine depletion process is more extensive than the first and culminates in the high-temperature desorption of an iron chloride species (also shown later), leading to loss of all Cl from the surface at ~1000 K.

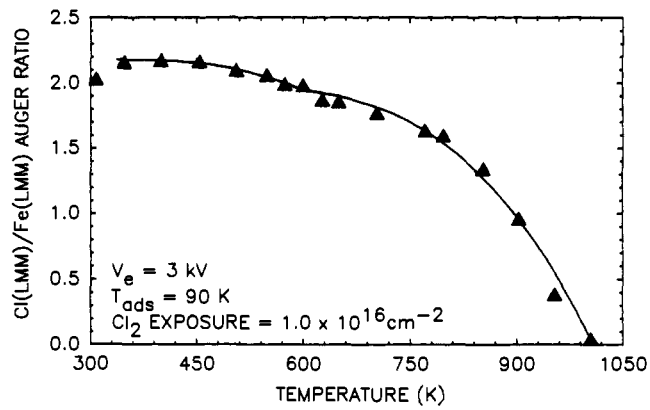

Figure 8. Plot of Cl(LMM)/Fe(LMM) Auger ratio, as a function of temperature, obtained at 90 K, following the adsorption of 1.0×10^{16} Cl_2/cm^2.

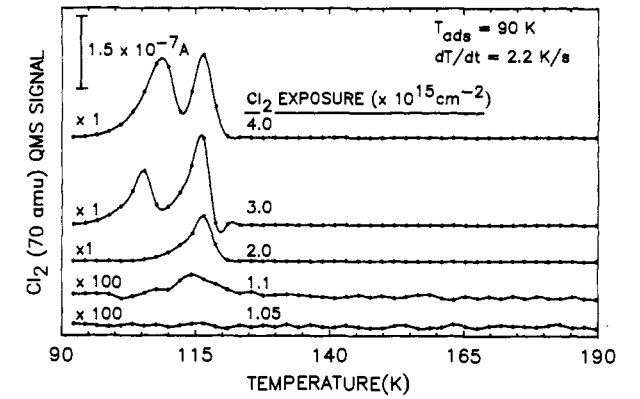

Figure 9. Temperature-programmed desorption spectra of undissociated Cl_2 from Fe(110), following adsorption of low exposures of Cl_2 on the surface at 90 K.

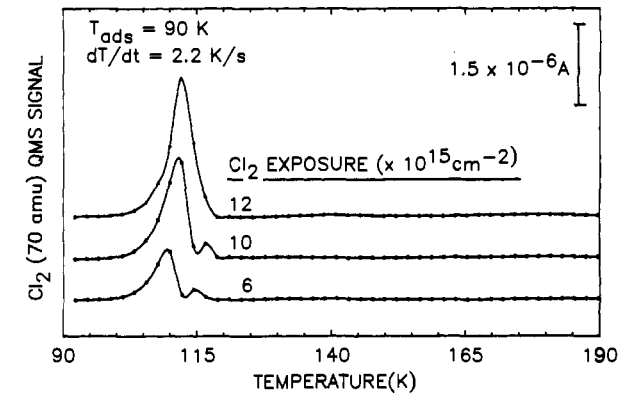

Figure 10. Temperature-programmed desorption spectra of undissociated Cl_2 on Fe(110), following adsorption of high exposures of Cl_2 on the surface at 90 K.

2. Thermal Desorption Measurements. 2.1. Thermal Desorption of Molecular Cl_2. The temperature-programmed desorption spectra for Cl_2 molecules adsorbed on the Fe(110) surface at 90 K are displayed in Figures 9 (low coverage) and 10 (high coverage). A molecular Cl_2 desorption process is not observed until the Cl_2 exposure is between 1.05 and 1.1×10^{15} Cl_2/cm^2, where a single desorption state appears at ~115 K. The absence of a molecular Cl_2 desorption state below a Cl_2 exposure of 1.1×10^{15} Cl_2/cm^2 indicates that Cl_2 adsorbs dissociatively at low exposures

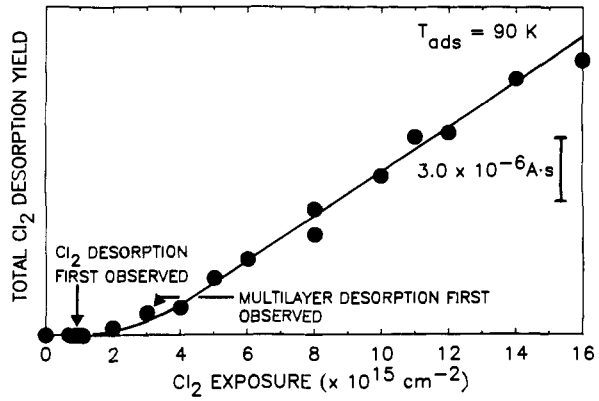

Figure 11. Plot of total Cl_2 desorption yield vs Cl_2 exposure. The plot indicates the first observation of Cl_2 desorption and multilayer desorption.

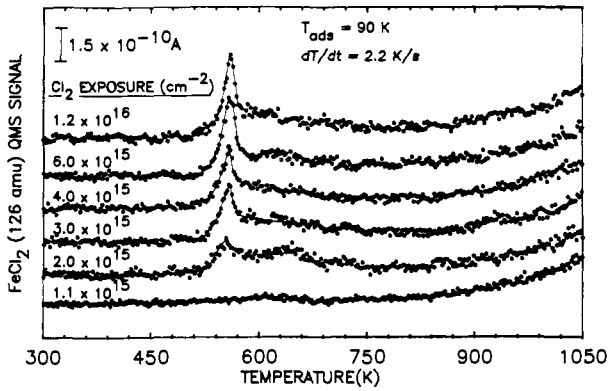

Figure 12. Temperature-programmed desorption of $FeCl_2$ following adsorption of Cl_2 on Fe(110) at 90 K. The desorption process at 560 K occurs via zero-order kinetics. The differences in heating programs for this experiment and the Auger experiment shown in Figure 8 are responsible for the presence of continued mass spectrometric detection of $FeCl_2$ desorption at 1050 K, compared to complete Cl depletion by Auger spectroscopy.

and that Cl_2 does not reform by Cl(a) recombination. At a Cl_2 exposure of 2.0 × 10^{15} Cl_2/cm^2, the intensity of the Cl_2 desorption state at ~115 K increases significantly, and the desorption peak temperature shifts to slightly higher temperatures. Initially, the yield of Cl_2 in the 115 K desorption state increases with increasing Cl_2 exposure. However, the yield in this state reaches saturation. At a Cl_2 exposure of 3.0 × 10^{15} Cl_2/cm^2, a second desorption state is observed at ~105 K. The desorption peak temperature for this second Cl_2 desorption state shifts to ~112 K at higher exposures as shown in Figure 10. The intensity of the state continues to increase as the Cl_2 exposure is increased, indicating that it corresponds to desorption from multilayers of Cl_2.

Figure 11 is a plot of the total integrated Cl_2 desorption yield from the Fe(110) crystal surface as a function of Cl_2 exposure at 90 K. The plot illustrates that the first molecular Cl_2 desorption is not observed until the Cl_2 exposure is 1.1 × 10^{15} Cl_2/cm^2, indicating that Cl_2 initially adsorbs dissociatively to produce a monolayer of Cl(a). When the monolayer of Cl(a) is complete, or essentially complete, a layer of molecular Cl_2 may be weakly held on top of Cl(a). This layer also saturates and then a multilayer of Cl_2 forms. As the multilayer desorption state is populated, the Cl_2 desorption yield increases linearly with increasing exposure, without reaching a constant value up to the highest exposure studied, 1.6 × 10^{16} Cl_2/cm^2.

2.2. Thermal Desorption of Iron Chloride Species following Adsorption of Cl_2 at 90 K. The thermal desorption spectra of $FeCl_2$ from the Fe(110) crystal surface as a function of Cl_2 exposure at 90 K are shown in Figure 12. At a Cl_2 exposure of 1.1 × 10^{15} Cl_2/cm^2, only a high-temperature iron chloride desorption state is present. This desorption process begins at ~900 K and continues to above 1050 K, the highest temperature studied (the phase transition from bcc to fcc occurs at 1183 K for iron[14] and places

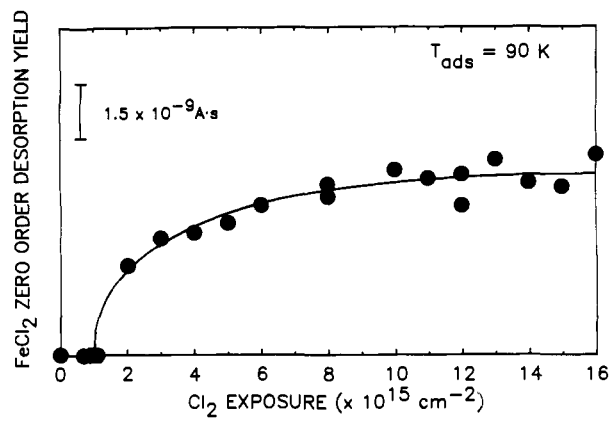

Figure 13. Plot of $FeCl_2$ zero-order desorption yield vs Cl_2 exposure at 90 K. Note saturation of $FeCl_2$ zero-order desorption yield above a Cl_2 exposure of ~1.0 × 10^{16} Cl_2/cm^2.

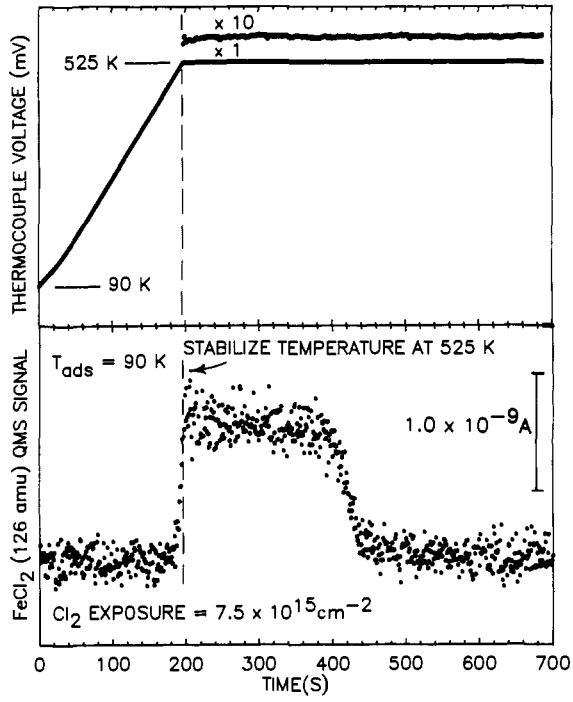

Figure 14. Isothermal desorption of $FeCl_2$ following adsorption of 7.5 × 10^{15} Cl_2/cm^2 on the defect-saturated Fe(110) surface. The temperature was stabilized at 525 K without further deviation in temperature (as shown by the top panel).

an upper limit on the temperature utilized). This high-temperature desorption state is attributed to an iron chloride species other than $FeCl_2$, based on the mass spectrometer cracking pattern which it exhibits. It could be nonequilibrated $FeCl_3$ which is thermodynamically unstable in the presence of Fe, or it could be Fe_2Cl_6.[4]

When the Cl_2 exposure is increased to 2.0 × 10^{15} Cl_2/cm^2, two additional desorption states are clearly observed at ~550 K and between 580 K < T < 750 K. This is in general agreement with results obtained on polycrystalline iron.[2] The intensity of the 550 K desorption state increases and its peak maximum shifts to a slightly higher temperature (560 K) as the Cl_2 exposure is increased. Figure 13 shows that the yield of the 560 K desorption state reaches a constant value above a Cl_2 exposure of ~10 × 10^{15} Cl_2/cm^2. The intensity of the broad $FeCl_2$ desorption state between 580 and 750 K remains essentially constant for all the Cl_2 exposures studied above 1.1 × 10^{15} Cl_2/cm^2.

For experiments involving different Cl_2 exposures, it has been found that the leading edges of the 560 K $FeCl_2$ desorption traces

(14) Cotton, F. A.; Wilkinson, G. *Advanced Inorganic Chemistry—A Comprehensive Text*, 4th ed.; Wiley: New York, 1980; p 752.

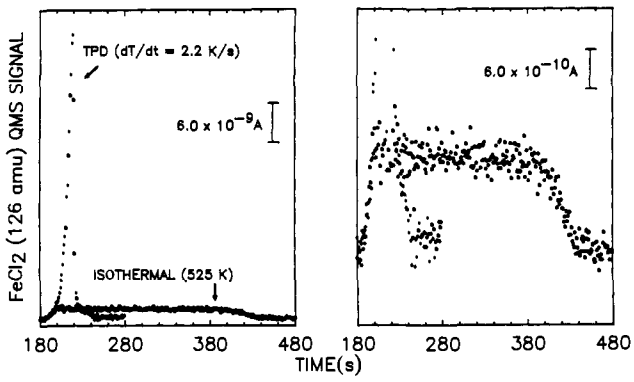

Figure 15. A comparison of the temperature-programmed desorption and the isothermal desorption of $FeCl_2$ showing accurate overlap of the leading edges of the two experiments. The total yield of $FeCl_2$ differs by only 10% between the two experiments.

accurately overlap as the initial chlorine coverage is increased. This is an indication that the 560 K $FeCl_2$ desorption process is governed by a rate law which is zero order in coverage.[9]

To verify the zero-order desorption of $FeCl_2$ (560 K), Figure 14 shows an isothermal desorption experiment for $FeCl_2$ following adsorption at 90 K on a defect-saturated surface (in the following section it will be shown that the desorption yield of $FeCl_2$ increases dramatically for a defect-saturated surface produced by ion bombardment). For this experiment, the crystal containing adsorbed chlorine was heated at a rate of 2.2 deg K/s until the temperature program was abruptly stopped at 525 K where the temperature was held constant throughout the desorption as shown in the upper panel of Figure 14. The isothermal desorption yield of $FeCl_2$ (lower panel, Figure 14) shows that the desorption rate for $FeCl_2$ remains essentially constant over time at 525 K. This independence of $FeCl_2$ desorption rate on surface coverage (indicating zero-order kinetics[9]) is observed up to a critical point in decreasing coverage where the desorption rate decreases rapidly near the end of the $FeCl_2$ desorption process. Therefore, $FeCl_2$ initially desorbs with zero-order kinetics. This zero-order process corresponds to sublimation from associated $FeCl_2$ species. This observation indicates that bulk $FeCl_2$ is present in localized regions on the surface.

A comparison of the isothermal desorption experiment (Figure 14) with TPD measurements of $FeCl_2$ from the defect-saturated Fe(110) surface is given in Figure 15 at two levels of vertical magnification. Here it may be seen that the leading edge of the $FeCl_2$ desorption trace overlaps precisely up to 525 K, where the temperature is stabilized in the isothermal measurements. The isothermal depletion (525 K) occurs at a constant rate over a time period of ~200 s, and the total yield of $FeCl_2$ measured in the two experiments agrees to within 10%.

To check that the zero-order desorption of $FeCl_2$ corresponds to sublimation of "bulk" $FeCl_2$, the standard enthalpy change for the zero-order process can be calculated using the Clausius–Clapeyron equation.[9,15] Here, data along the leading edge of the zero-order $FeCl_2$ desorption process below 560 K are analyzed. Figure 16 shows a plot of ln (desorption rate of $FeCl_2$) vs $1/T$ which yields a slope of -2.44×10^4 K corresponding to a value of 48.5 ± 1.2 kcal/mol for the enthalpy of sublimation of $FeCl_2$. The measured value of 48.5 ± 1.2 kcal/mol is in good agreement with the literature value of $\Delta H°_{sub}(FeCl_2(s))$ = 44.0 ± 3.0 kcal/mol,[16-20] as well as with the values reported for $FeCl_2$ zero-order desorption from CCl_4/Fe(110) (48.7 ± 8.2 kcal/mol)[4] and C_2Cl_4/Fe(110) (44.8 ± 8.5 kcal/mol).[21]

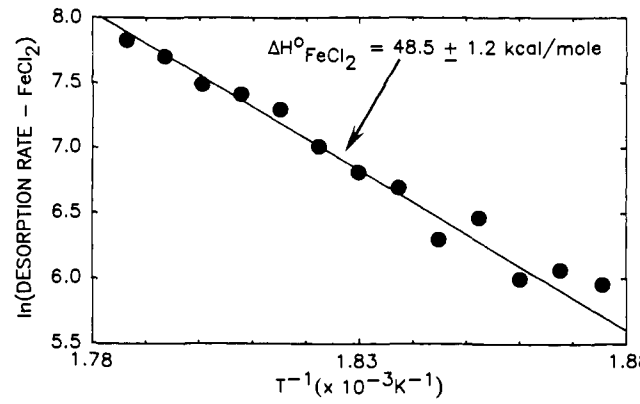

Figure 16. Plot of ln (desorption rate $FeCl_2$) vs $1/T$ for the $FeCl_2$ desorption at 560 K. A value of 48.5 ± 1.2 kcal/mol was obtained from this plot for the enthalpy of sublimation of $FeCl_2$.

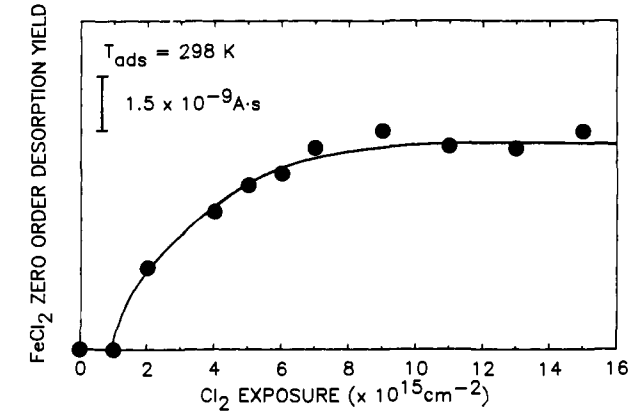

Figure 17. Plot of $FeCl_2$ zero-order desorption yield as a function of Cl_2 exposure at 298 K. Note that the $FeCl_2$ desorption yield reaches saturation at a Cl_2 exposure of $\sim 8 \times 10^{15}$ Cl_2/cm^2.

2.3. Cl_2 Adsorption at 298 K. Thermal desorption experiments were carried out for molecular Cl_2 and $FeCl_2$ from the Fe(110) crystal following Cl_2 exposure at 298 K. A molecular Cl_2 desorption process was not observed, indicating complete irreversible dissociative adsorption of Cl_2 at 298 K. Thermal desorption spectra for $FeCl_2$, following Cl_2 exposure at 298 K, revealed desorption features at 560 K, ~640 K, and high temperatures corresponding to those of the high-temperature iron chloride species. Figure 17 shows the $FeCl_2$ zero-order desorption yield as a function of increasing Cl_2 exposure at 298 K. The desorption state at 560 K for $FeCl_2$ from the Fe(110) surface appears to exhibit threshold exposure for Cl_2 of $\sim 1 \times 10^{15}$ Cl_2/cm^2 as was observed for Cl_2 adsorption at 90 K. The zero-order $FeCl_2$ desorption yield increases with increasing Cl_2 exposure and reaches a constant value at a Cl_2 exposure of $\sim 8 \times 10^{15}$ Cl_2/cm^2. The $FeCl_2$ desorption yield at saturation Cl_2 exposures is the same for Cl_2 exposures at 90 and 326 K.

2.4. Yield of Zero-Order $FeCl_2$ as a Function of Cl_2 Adsorption Temperature. Despite the fact that the comparison of Figures 13 and 17 would suggest that the yield of $FeCl_2$ does not depend on surface temperature during Cl_2 adsorption, it has been found that this generalization is not true. A series of adsorption experiments over the range 90–500 K (Figure 18) indicate a complex dependence of the $FeCl_2$ yield (560 K state) on the Fe(110) temperature when it receives Cl_2(g).

The first two points (in Region I of Figure 18), representing Cl_2 adsorption at 90 K, show that a high yield of $FeCl_2$ occurs when multilayer and monolayer Cl_2 are produced in the adsorption process at this temperature (the Cl_2 desorption is shown in Figure 10).

When Cl_2 adsorption occurs at 120 K (third point in region I of Figure 18), the yield of $FeCl_2$ is significantly lower compared

(15) Atkins, P. W. *Physical Chemistry*, 2nd ed.; W. H. Freeman and Co.: San Francisco, 1982; p 189.
(16) Kabaschewski, O.; Evans, E. L.; Alcock, C. B. *Metallurgical Thermochemistry*; Pergamon Press: New York, 1967.
(17) Kelley, K. K. Critical Evaluations of Vapor Pressures and Heats of Evaporation of Inorganic Substances. Bull-U.S. Bur. Mines 1935, No. 383.
(18) Schafer, H. Z. *Anorg. Allg. Chem.* **1955**, *178*, 300.
(19) Schoonmaker, R. C.; Porter, R. F. *J. Chem. Phys.* **1958**, *29*, 116.
(20) Sime, R. J.; Gregory, N. W. *J. Phys. Chem.* **1960**, *64*, 86.
(21) Smentkowski, V. S.; Yates, J. T., Jr. *Surf. Sci.* **1989**, *220*, 307.

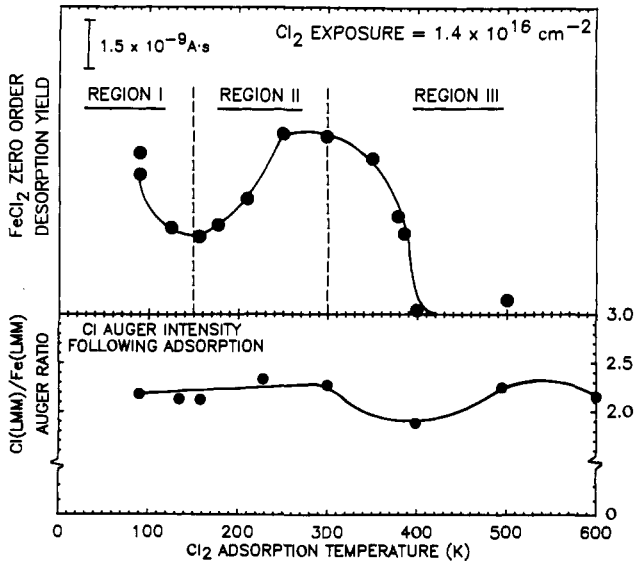

Figure 18. $FeCl_2$ zero-order desorption yield as a function of Cl_2 adsorption temperature. See text for discussion. The lower panel shows that the Auger ratio remains essentially constant over the Cl_2 adsorption temperature range.

to the first two points at 90 K. This third point corresponds to a Cl_2 adsorption process at a surface temperature where stable Cl_2 adsorbate is not present on the Fe(110) crystal surface.

As the Cl_2 adsorption temperature is raised above 150 K (region II of Figure 18), the yield of zero-order $FeCl_2$ begins to increase, reaching a maximum near 300 K. Above 300 K (region III of Figure 18), the yield of $FeCl_2$ again begins to decrease, and for Cl_2 adsorption at a crystal temperature of ~400 K, no zero-order $FeCl_2$ is produced.

These results suggest that the production of zero-order $FeCl_2$ is strongly kinetically dependent on surface processes which turn off, turn on, and then turn off as the surface temperature is raised from 90 to 400 K. These variations in $FeCl_2$ yield occur under conditions where the Cl Auger intensity is virtually constant following Cl_2 adsorption at the different surface temperatures as shown in the bottom panel of Figure 18. Possible explanations are presented in the Discussion concerning this complex behavior.

3. Defect Production by Ar^+ Bombardment of the Fe(110) Surface. Defects were produced, in a controlled manner, on the clean Fe(110) crystal by Ar^+ bombardment. The degree of surface disorder was measured in monolayers of Ar^+ incident. The total charge received by the crystal (area = 0.20 cm^2) was measured and converted to monolayers of Ar^+ incident (1 ML Ar^+ incident = 1.72×10^{15} Ar^+/cm^2 = 2.8×10^{-4} C/cm^2).

3.1. Thermal Desorption of $FeCl_2$ following Surface Defect Enhancement on Fe(110). Following defect production, the Fe(110) crystal was exposed to 1.0×10^{16} Cl_2/cm^2 at 90 K and a line-of-sight temperature-programmed desorption experiment was carried out. Figure 19 shows the $FeCl_2$ zero-order desorption yield as a function of monolayers of Ar^+ incident. Increasing the coverage of surface defects by Ar^+ bombardment increases the $FeCl_2$ zero-order desorption yield at 560 K very significantly. Above 0.2 ML of Ar^+ incident, the yield of the $FeCl_2$ desorption process becomes essentially constant due to maximum defect production; further Ar^+ bombardment of the crystal prior to Cl_2 adsorption has no effect on the $FeCl_2$ production. The desorption yield increases by a factor of 9.2 going from a nonbombarded surface to a defect-saturated surface.

Temperature-programmed desorption experiments were also carried out on a clean and a defect-saturated Fe(110) surface followed by adsorption of 1.0×10^{16} Cl_2/cm^2 at 137 K. At 137 K, multilayers of molecular Cl_2 do not adsorb on the iron surface and the temperature is not high enough to completely anneal out the defects produced by Ar^+ bombardment.[22] As shown by the

(22) Smentkowski, V. S.; Yates, J. T., Jr. *Surf. Sci.* **1990**, *232*, 102.

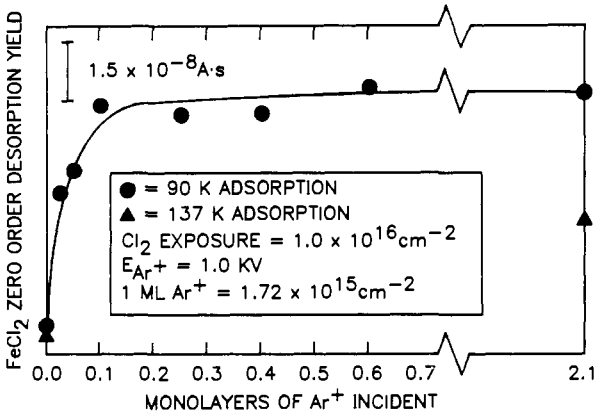

Figure 19. Plot of $FeCl_2$ zero-order desorption yield as a function of monolayers of Ar^+ incident. Surface defect saturation is obtained at ~0.2 monolayer at Ar^+ incident.

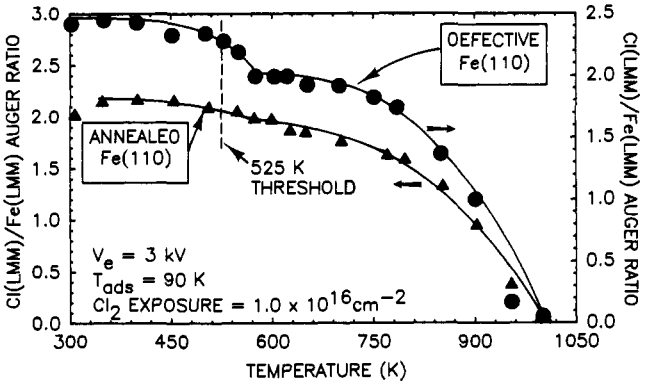

Figure 20. Comparison of the Cl(LMM)/Fe(LMM) Auger ratio as a function of temperature for a defect-saturated and an annealed Fe(110) surface. Note the difference in the y-axis scales for the two plots. The error in the measurements is represented by the size of the symbols.

two triangles in Figure 19, the $FeCl_2$ zero-order desorption yield also increases when a defect-saturated surface adsorbs chlorine at 137 K.

3.2. Auger Spectroscopic Studies of the Thermal Behavior of Chlorine Layers on a Defect-Saturated Fe(110) Surface. A study of chlorine Auger intensity as a function of temperature was also conducted on a defect-saturated surface exposed to 1.0×10^{16} Cl_2/cm^2. The procedure used in section III-1.4 was followed for the defect-saturated surface. Figure 20 is a comparison of the Cl(LMM)/Fe(LMM) Auger ratio as a function of temperature for the annealed and defect-saturated surfaces. Two thermal depletion processes are clearly evident for the annealed and defect-saturated surfaces. However, the defect-saturated surface displays an enhanced Cl(LMM)/Fe(LMM) Auger ratio decrease in the temperature range 450–570 K. This agrees quite well with the increase in the yield of the zero-order 560 K $FeCl_2$ desorption state observed by mass spectroscopy and serves to associate the Auger behavior below 570 K with effects on defect sites.

IV. Discussion

1. Mechanism for Adsorption of Cl_2 at 90 K. Three adsorption states exist for Cl_2 on Fe(110) at 90 K. An initial Cl_2 exposure to the iron surface adsorbs dissociatively and irreversibly at 90 K. The Cl(a) dissociated species lead to oxidation of the iron surface, indicated by the presence of line shape changes in the Fe(MVV) transition of the Auger spectrum which are similar to the line shape change observed when oxygen was dissociatively adsorbed on Fe(110), oxidizing the surface.[13] Thus the first layer of chemisorbed Cl is considered to be schematically represented as $Cl^{\delta-}(a)$.

When a monolayer of $Cl^{\delta-}(a)$ is complete, a layer of weakly-chemisorbed Cl_2 molecules (or possibly adsorbed Cl atoms) adsorbs on top of the $Cl^{\delta-}(a)$ fragments. Multilayers of Cl_2 (present as a Cl_2 ice) then form over the layer of weakly-chemisorbed Cl_2

molecules. A molecular Cl_2 desorption state for the weakly-chemisorbed $Cl_2(a)$ layer is first observed at 117 K at a Cl_2 exposure of 1.1×10^{15} Cl_2/cm^2. The desorption temperature observed for the weakly-chemisorbed $Cl_2(a)$ molecules is influenced by the presence of an induced dipole in the $Cl_2(a)$ layer resulting from dipoles present in the underlayer of $Cl^{\delta-}(a)$ fragments. The weakly-chemisorbed $Cl_2(a)$ molecular desorption state occurs at a higher temperature than the desorption state observed for the multilayers of Cl_2.

The multilayer Cl_2 desorption state is evolved with a desorption rate maximum at ~112 K at Cl_2 exposures higher than 3.0×10^{15} Cl_2/cm^2. This Cl_2 multilayer desorption state increases in coverage with increasing exposure, and its kinetic behavior is indicative of zero-order kinetics.[9] Therefore, the activation energy for desorption can be compared to the enthalpy of sublimation of $Cl_2(s)$ at 112 K. The activation energy for desorption was determined from the leading edge of the Cl_2 desorption curve using the Clausius–Clapeyron equation.[9,15] The value obtained from the plot of ln (P) vs $1/T$ for the activation energy for desorption is 8.8 ± 0.9 kcal/mol. This measured value compares with the calculated value of 6.77 kcal/mol for the ΔH°_{sub} (enthalpy of sublimation) of $Cl_2(s)$ at 112 K. This value was calculated from the enthalpy of fusion,[23] the enthalpy of vaporization,[23] and the heat capacities for the solid, liquid, and gas[23,24] phases of Cl_2.

2. Mechanism for Adsorption of Cl_2 at 298 K. Cl_2 adsorbs dissociatively on Fe(110) with an initial constant (and probably near unity) sticking probability as shown by the linear section of the curve in Figure 3. This observation indicates the presence of a mobile Cl_2 precursor state[25] where weakly-adsorbed $Cl_2(a)$ feeds the Cl(a) dissociated species state.

A line shape change in the Fe(MVV) Auger transition for Cl_2 adsorption at 298 K, similar to that observed for adsorption at 90 K, shows that dissociative adsorption of Cl_2 to produce $Cl^{\delta-}(a)$ species at 298 K leads to oxidation of the Fe(110) surface.

3. Thermal Desorption of $FeCl_2$ Species Produced from Cl_2 Adsorption at 90 K. The TPD process observed for $FeCl_2$ at 560 K (Figure 12) and the isothermal desorption experiment performed for $FeCl_2$ following adsorption of Cl_2 at 90 K (Figures 14 and 15) both show that the $FeCl_2$ desorption rate for the thermal desorption process is independent of surface coverage. This observation indicates that at temperatures near 560 K, $FeCl_2$ desorbs with zero-order kinetics. The kinetics and energetics of this process correspond closely to the sublimation of bulk $FeCl_2$. The value obtained from a leading edge analysis of the 560 K $FeCl_2$ desorption process is 48.5 ± 1.2 kcal/mol which is in good agreement with the literature value of 44.0 ± 3.0 kcal/mol[16-20] for the enthalpy of sublimation of bulk $FeCl_2$.

The observation that the $FeCl_2$ zero-order desorption state at 560 K is detected at low Cl_2 exposures where multilayer Cl_2 is not present indicates that only a relatively small quantity of Cl is needed to form the $FeCl_2$ species. The fact that $FeCl_2$ desorbs with zero-order kinetics at 560 K at low Cl_2 exposures *suggests that zero-order kinetics are not the result of the presence of a dispersed multilayer of $FeCl_2$*. Rather, it is postulated that $FeCl_2$ forms clusters (reminiscent of small multilayer regimes) at defect nucleation sites on the Fe(110) surface. This argument was tested using controlled Ar^+ bombardment to produce artificial defect sites on the Fe(110) surface prior to Cl_2 adsorption. Figure 19 shows that increasing the defect density (and therefore the number of defect nucleation sites) dramatically increases the $FeCl_2$ zero-order desorption yield. After the crystal has been exposed to ~0.2 ML Ar^+ incident, the $FeCl_2$ desorption yield saturates which indicates that the Fe(110) surface is saturated with defect nucleation sites.

The initial defect density present on the nonbombarded Fe(110) crystal used in this work is smaller than the initial defect density on another nonbombarded Fe(110) crystal used in previous work.[22]

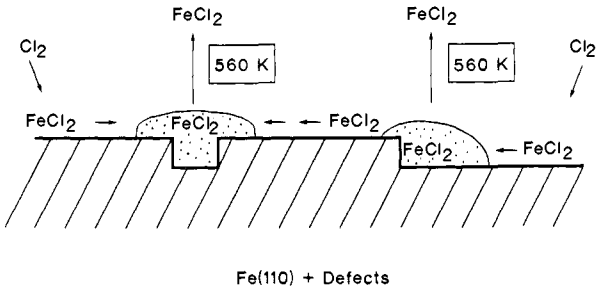

Figure 21. Illustration of $FeCl_2$ clustering at defect locations on the Fe(110) surface following adsorption of chlorine. The clusters produce ~6% screening of the chlorine Auger signal.

Therefore, the increase in the $FeCl_2$ yield for a defect-saturated surface produced by Ar^+ bombardment is ~5 times greater here than that reported previously.[22]

4. Estimation of $FeCl_2$ Cluster Size from Auger Attenuation. Auger spectroscopic measurements on the defect-saturated Fe(110) surface show that the Cl(LMM)/Fe(LMM) Auger ratio starts to decrease at ~400 K and reaches a singularity at ~570 K (Figure 20). Mass spectroscopy shows that there are no products containing chlorine that desorb in the temperature range ~120 K < T < ~500 K (Figures 9, 10, and 12). It is therefore postulated that at ~400 K, $FeCl_2$ species start to nucleate at defect sites on the Fe(110) surface. This nucleation process results in a ~6% decrease in the Cl(LMM)Fe(LMM) Auger ratio from 400 to 525 K. The chlorine located inside the $FeCl_2$ clusters is shielded (and therefore the chlorine Auger intensity is attenuated) by overlayers of $FeCl_2$ in the cluster. A simple attenuation model can be employed to approximately estimate the minimum thickness of the clusters assuming that all Cl atoms participate in clustering. The relationship between the reduction in Auger intensity for chlorine and the thickness of the clusters is given as

$$\frac{I}{I_0} = \frac{\lambda[1 - e^{-d/\lambda}]}{d} \qquad (1)$$

where I/I_0 is the final over initial Cl(LMM)/Fe(LMM) Auger ratio, d is the thickness of the clusters in angstroms, and λ is the attenuation length (in angstroms) for a 180-eV electron through a solid $FeCl_2$ layer.

The attenuation length (λ) was obtained from the TPP-2 general formula for the inelastic mean free path (IMFP).[26] A 20% error for the IMFP was considered when the determination of λ was reported. The attenuation length is between 15 and 35% less than the calculated IMFP[26,27] (which depends on the differential cross sections for elastic scattering and therefore on atomic number and electron energy). Using eq 1, the cluster thickness (d) was calculated to be between 2.8 and 5.4 Å using a λ range of 3.1–6.0 Å for an electron traveling through a bulk $FeCl_2$ layer with 180-eV energy. If only a fraction of the surface Cl participates in cluster formation, as is likely, then the average cluster thickness, d, will be larger than that estimated here.

It is of interest to compare the estimated cluster thickness of $FeCl_2$ with the crystal structure of solid $FeCl_2$. $FeCl_2$ crystallizes as a layered solid consisting of $FeCl_2$ sheets in which the exterior Cl^- ions interact with neighbor sheets. The interplanar distance between Fe^{2+} ions in this sheet structure is 5.84 Å.[28,29] Figure 21 schematically illustrates the clustering of $FeCl_2$ at defect sites on the Fe(110) surface in a layer-or-two fashion to produce ~6% Auger screening.

A second chlorine depletion process begins at ~720 K and continues to 1000 K. This process may also involve a second stage

(23) Giauque, W. F.; Powell, T. M. *J. Am. Chem. Soc.* **1939**, *61*, 1970.
(24) Lewis, G. N. *Thermodynamics*, 2nd ed.; McGraw-Hill Book Co., Inc: New York, 1961; p 66.
(25) Weinberg, W. H. In *Kinetics of Interface Reactions*; Grunze, M., Kreuzer, H. J., Eds.; Springer-Verlag: New York, 1987; p 94.
(26) Tanuma, S.; Powell, C. J.; Penn, D. R. *J. Vac. Sci. Technol.* **1990**, *A8* (*3*), 2213.
(27) Powell, C. J. *J. Electron Spectrosc. Relat. Phenom.* **1988**, *47*, 197.
(28) Ferrari, A.; Celeri, A.; Giorgio, F. In *Strukturbericht*; Hermann, C., Lohrmann, O., Phillipp, H., Eds.; Edward Brothers, Inc.: Ann Arbor, 1943; Vol. 2, p 245.
(29) Ewald, P. P.; Hermann, C., Eds. In *Strukturbericht*; Edward Brothers, Inc.: Ann Arbor, 1943; Vol. 1, p 742.

of iron chloride nucleation, followed by desorption.

5. Comparison of the Results Obtained for Cl_2 with Chlorinated Organic Reactants on Fe(110). Interesting trends are observed when the chemical reactivity of a simple halogen molecule (Cl_2) on the Fe(110) surface is compared and contrasted with that of chloroalkane and chloroalkene molecules (CCl_4,[4] C_2Cl_4,[21] and CCl_2F_2[30]) on the same surface. In all four cases, corrosive chemisorption from molecular decomposition is observed when the clean iron surface is exposed to low coverages at 90 K. When the coverage is increased, monolayer and multilayer desorption processes for the undissociated molecules occur.

For each molecule studied, zero-order iron dihalide production is observed upon temperature-programmed desorption after the crystal is exposed to the molecule at 90 K. For Cl_2, CCl_4,[4] and C_2Cl_4,[21] the iron dihalide is $FeCl_2$ which desorbs in each case at 560 K. In contrast, for CCl_2F_2,[30] the iron dihalide corresponds solely to FeF_2 which desorbs at ~730 K (no $FeCl_2$ desorption is observed). When the defect density on the Fe(110) surface is increased by Ar^+ bombardment, the zero-order iron dihalide desorption yield is enhanced following adsorption for Cl_2, CCl_4,[22] and CCl_2F_2.[22] Thus, all of these halogen-bearing molecules lead to $FeCl_2$ (FeF_2) production at metal defect sites.

The broad iron chloride desorption state observed at 580 K < T < 750 K for Cl_2/Fe(110) was not observed for CCl_4/Fe(110)[4] or C_2Cl_4/Fe(110),[21] although for the CCl_2F_2/Fe(110)[30] system a broad FeF_2 desorption state was observed at temperatures slightly greater than the FeF_2 zero-order desorption state at 730 K.

A high-temperature (T > 900 K) iron chloride desorption process is observed for all four molecules studied. This desorption state seems to be insensitive to the particular chlorine-containing molecule employed and to the temperature of adsorption employed.

In other work, it has been shown that increasing the amount of pre-adsorbed oxygen prior to CCl_4[31] and Cl_2[32] adsorption at 90 K causes the yield of the $FeCl_2$ zero-order desorption state to decrease.[31,32] It is interesting to note that when carbon-containing molecules are adsorbed onto Fe(110) at 300 K,[4,21,30] the zero-order $FeCl_2$ desorption process is not observed. This phenomenon may result from preferential C deposition at defect sites which therefore prevents $FeCl_2$ formation. This hypothesis was tested in the following experiment.

A second Fe(110) crystal was accidentally heated above the bcc to fcc phase transition. In the process carbon migrated to the surface from the bulk. On the basis of carbon Auger intensity measurements and Auger sensitivity factors,[33] 12 atomic % carbon was present in the surface region sampled by Auger spectroscopy. The iron surface with atomic carbon was then exposed to Cl_2 at 300 K. After the crystal was cooled to 90 K, a TPD experiment was performed. The zero-order $FeCl_2$ desorption yield at 560 K decreased by a factor of 3.2 compared to the same experiment performed on an atomically clean and annealed bcc surface. A decrease in the $FeCl_2$ desorption yield indicates that surface carbon does inhibit the formation of associated $FeCl_2$ species and the subsequent desorption of these species.

6. Cl_2 Adsorption Temperature Effects. The kinetics of $FeCl_2$ production from Cl_2 adsorption are strongly temperature dependent, as shown in Figure 18. The $FeCl_2$ desorption yield curve can be separated into three regions. In region I, there is a high coverage of Cl_2 at 90 K in the precursor state leading to a significant yield of $FeCl_2$ as forced by surface concentration effects. As the Cl_2 adsorption temperature is increased to 150 K, the $FeCl_2$ production diminishes due to the absence of the high coverage of Cl_2 in a precursor state. Region II shows that the yield of $FeCl_2$ is enhanced when the temperature of adsorption is increased from 160 to 300 K, where the yield of $FeCl_2$ becomes roughly equivalent to the yield at 90 K. The reason for this increase in region II is unknown at present. When the surface temperature for Cl_2 adsorption is greater than 300 K, region III, the production of $FeCl_2$ declines. The reason for this loss of $FeCl_2$ in region III is unknown at present.

V. Summary and Conclusions

The interaction of chlorine with Fe(110) has been studied using thermal desorption and Auger spectroscopy measurements in the temperature range 90–1050 K. The following results were obtained:

1. Cl_2 initially adsorbs dissociatively and irreversibly at 90 K and oxidizes the Fe(110) surface as observed by Auger line shape changes. The production of $Cl^{\delta-}$(a) species is postulated.

2. A layer of weakly chemisorbed molecular Cl_2 adsorbs on top of the layer of dissociated $Cl^{\delta-}$(a) species. A molecular Cl_2 desorption process is observed for the weakly-chemisorbed Cl_2 in this second layer at 117 K.

3. Multilayers of Cl_2(s) form (as a Cl_2 ice) over the layer of weakly-chemisorbed molecular Cl_2(a). Cl_2 desorbs from the multilayer with zero-order kinetics at a temperature of 112 K, as sublimation occurs from the Cl_2(s) layer. $\Delta H_{sub} = 8.8 \pm 0.9$ kcal/mol for this thermal desorption process.

4. The interaction of Cl_2 with Fe(110) produces $FeCl_2$.

5. TPD experiments and isothermal desorption experiments show that the desorption process at 560 K for $FeCl_2$ takes place via zero-order kinetics. The enthalpy of sublimation calculated for the process is 48.5 ± 1.2 kcal/mol. This process is postulated to occur from $FeCl_2$ clusters on natural defect sites on the Fe(110) surface.

6. Auger spectroscopic measurements on a defect-saturated surface as a function of temperature show a decrease in the chlorine signal prior to the $FeCl_2$ zero-order desorption temperature. This is postulated to result from $FeCl_2$ cluster formation and related self screening by $FeCl_2$ in the Auger measurements. A simple attenuation model was used to estimate the thickness of the $FeCl_2$ clusters to be in the approximate range 2.8–5.4 Å.

7. A defect-saturated iron surface produced by Ar^+ bombardment exhibits a significantly enhanced yield of the zero-order $FeCl_2$ process at 560 K. This effect supports the model that $FeCl_2$ forms clusters at defect sites.

8. A broad $FeCl_2$ desorption process is observed between 580 K < T < 750 K, even at low Cl_2 exposures. This broad desorption process is attributed to desorption of $FeCl_2$ from a dispersed layer.

9. A high-temperature desorption process (T > 900 K) is observed even at low Cl_2 exposures and is due to the desorption of an iron chloride species other than $FeCl_2$ that forms due to the dissociative adsorption of Cl_2.

10. The kinetics involved in the production of $FeCl_2$ are definitely temperature dependent. A decrease in $FeCl_2$ yield is observed between 90 and 150 K. This is postulated to be due to a reduction in the surface coverage of a Cl_2 precursor to chemisorption. An increase in $FeCl_2$ yield is then observed at Cl_2 adsorption temperatures between 150 and 300 K which is unexplained at present. Finally, the $FeCl_2$ yield decreases again, for adsorption temperatures in the range 300–400 K, and this is unexplained at present.

11. The existence of surface carbon prior to the adsorption of Cl_2 decreases the $FeCl_2$ desorption yield. This is probably related to inhibition of dissociative Cl_2 adsorption on surface defects by the adsorbed carbon.

Acknowledgment. We gratefully acknowledge support of this work by 3M Corporate Research Laboratory. Helpful discussions with Dr. David Broberg are acknowledged.

Registry No. Cl_2, 7782-50-5; Fe, 7439-89-6; $FeCl_2$, 7758-94-3.

(30) Smentkowski, V. S.; Yates, J. T., Jr. *Surf. Sci.* **1990**, *232*, 92.
(31) Smentkowski, V. S.; Ellison, M. D.; Yates, J. T., Jr. *Surf. Sci.* **1990**, *235*, 116.
(32) Linsebigler, A. L.; Smentkowski, V. S.; Yates, J. T., Jr. Submitted for publication.
(33) Davis, L. E.; MacDonald, N. C.; Palmberg, P. W.; Riach, G. E.; Weber, R. E. *Handbook of Auger Spectroscopy*, 2nd ed.; Physical Electronics Division, Perkin Elmer Co.: Eden Prairie, 1978.